All-optical electron spin quantum computer with ancilla bits for operations in each coupled-dot cell

Toshio Ohshima
Fujitsu Laboratories Ltd., 10-1 Morinosato-Wakamiya, Atsugi 243-0197, Japan
(Received 12 May 2000; published 15 November 2000)

A cellular quantum computer with a spin qubit and ancilla bits in each cell is proposed. The whole circuit works only with the help of external optical pulse sequences. In the operation, some of the ancilla bits are activated, and autonomous single-and two-qubit operations are made. In the sleep mode of a cell, the decoherence of the qubit is negligibly small. Since only two cells at most are active at once, the coherence can be maintained for a sufficiently long time for practical purposes. A device structure using a coupled-quantum-dot array with possible operation and measurement schemes is also proposed.

PACS number(s): 03.67.Lx, 73.61.−r

Since the formulation of the quantum computer and quantum circuit [1], theoretical studies on quantum computers have clarified their efficiency in highly complex computational tasks; factorization and search are two examples [2–4]. Some physical implementations have been proposed. Moreover, their operations on a few qubits have been demonstrated experimentally [5–13]. Although these studies are impressive, these systems (e.g., liquid nuclear magnetic resonance, ion trap, linear optics) are not promising since they are limited in their possible integration: 10 qubits or thereabouts.

Thus, a quantum computer based on conventional semiconductor technology has been expected. Kane proposed a silicon-based qubit using the nuclear spin of a phosphorus donor [14]. Although this idea has the additional advantage of good isolation of nuclear spins from the environment, it requires precise position control of individual impurities. On the other hand, qubits based on the electrons in semiconductor nanostructures are more realistic since, nowadays, quasi-zero-dimensional quantum dots can be fabricated with high feasibility using various techniques. Furthermore, the control of the motion of individual electrons in such structures has also proved to be possible using single-electron effects.

In 1995, Barenco *et al.* proposed a quantum-dot-based implementation [15]. They utilized the quantized energy levels in a quantum dot as two states of a qubit. The Coulomb interaction between dipole moments of two adjacent dots induced by an externally applied electric field was used for the controlled NOT operation. Discrete atomlike and moleculelike levels in quantum dots have been observed experimentally [16–18]. It should become possible to control the quantum states coherently from outside. However, in general, the decoherence of electron wave functions in excited levels is fast since they are strongly coupled to the electromagnetic and acoustic environment. Quantum error correction and fault-tolerance theories have shown that some amount of decoherence can be overcome [19–27]. However, a sufficiently large time ratio R_t of coherence time to gating time is required in order for the correction procedures to be effective. The simple quantum dot scheme does not fulfill this criterion.

In 1998, Loss and DiVincenzo proposed to use the spin of an electron confined in a quantum dot [28,29]. The spin degree of freedom is expected to be well isolated from photon and phonon environments. Furthermore, the two-qubit operation is performed by simple spin exchange dynamics instead of the usual controlled NOT. This operation is virtually a two-electron quantum beat, which is switched on by lowering the barrier between two quantum dots to allow interdot tunneling. The two spins of the quantum dots are exchanged continuously in time. This scheme, however, has difficulty in the modulation of the barrier. Magnetic gating has a disadvantage in the operational speed, which eventually reduces the time ratio. Gating by nanoscale electrodes requires an extremely advanced fabrication technology.

In this paper, we propose an all-optical implementation scheme for a quantum-dot-based quantum circuit that has the cellular structure of a spin qubit and m ancilla bits in each cell. In our scheme, single- and two-bit operations are performed if and only if specific ancilla bits are excited (the active state of a cell). In the ground state of a cell, no operation is performed (the sleeping state of a cell). Therefore, in sleeping cells, coherence is maintained very faithfully. Since the duty ratio of active time to total time scales as N^{-1}, the effective time ratio becomes N times larger.

Our scheme is not restricted to a particular physical system. It may be feasible in molecular quantum computers or trapped-ion systems. However, we focus here on the more promising quantum-dot-based implementation. Transitions between quantum levels of coupled quantum dots with and without external electromagnetic field have been observed in the experiments by Fujisawa *et al.* [17] and Oosterkamp *et al.* [18]. They used high-mobility two-dimensional electron systems formed at heterojunctions. By lateral confinement using patterned electrodes or inactivation using focused ion beam implantation, zero-dimensional quantum dots (or disks) of about 100 nm in diameter are formed. Without an external electromagnetic field, it has been shown that the transition rates between levels obey a simple relation that is consistent with the usual model of the interaction with the bosonic reservoir. On the other hand, when an external electromagnetic field (microwave signal) of less than 50 GHz is applied, a strong transition is possible only when the frequency is resonant with the level spacings. The tunnel couplings between quantum dots can be continuously changed by an electrode or magnetic field. When the coupling is

weak, the transition is photon-assisted tunneling between quantum states well localized in each dot. Multiphoton processes involving up to 11 photons have been observed. When the coupling is strong, single-photon absorptions between bonding and antibonding states of two dots have been observed. This indicates that coherent quantum states extending over two spatially separated dots exit. The decoherence time of quantum states has been estimated to be about 1 ns. Thus, in a quantum-dot system, an electron spin qubit is equipped with an ancilla bit only by locating another dot in the proximity of the main dot. Our cell is made of $m+1$ weakly coupled dots. To have the lowest energy level, the main dot has the largest size. The material with the lowest conduction band edge may be used instead. The main dot is surrounded by m ancilla dots of different sizes and different energy levels E_k, $k=1,...,m$. Resonant optical π pulses transfer electrons from the main dot to a specific ancilla dot, and vice versa. The cell state is denoted by $|w, k\rangle$, where the integer k stands for the dot in the cell that contains the electron. That is, we utilize the ancilla not as a vector in $(m+1)$-dimensional Hilbert space but as a classical $(m+1)$-state system. We will explain this idea of Hilbert space contraction later.

The whole system is a one-, two-, or three-dimensional network of these kinds of cell. Each cell has a definite number of connections to neighboring cells. Let us define the interaction between two neighboring cells: cell a and cell b. The interaction is switched on if and only if the ancilla states of these cells are k and l, respectively:

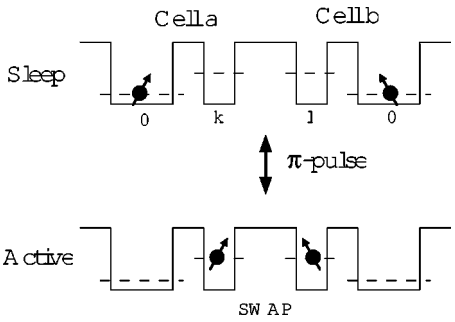

FIG. 1. The selective interaction between cell a and cell b by real space transfers of electrons into the kth and lth ancillas due to an optical π pulse.

$$\{|a\rangle=|w_a,k\rangle_a\}\wedge\{|b\rangle=|w_b,l\rangle_b\} \tag{1}$$

where k and l are specific numbers for pair a and b. We designed this such that $E_k(\text{cell}\,a)=E_l(\text{cell}\,b)$. This selective interaction can be realized by the real space transfer of electron wave functions due to the transition in ancilla bits. In other words, two electrons in two cells approach each other under this specific condition (Fig. 1).

The interaction may be of any kind. However, spin exchange is thought to be useful in this scheme. The unitary operator $U_{ab}(\theta)$ becomes

$$U_{ab}(\theta):\begin{cases}|0,k\rangle_a\otimes|0,l\rangle_b\mapsto|0,k\rangle_a\otimes|0,l\rangle_b\\ |0,k\rangle_a\otimes|1,l\rangle_b\mapsto\cos\theta|0,k\rangle_a\otimes|1,l\rangle_b-i\sin\theta|1,k\rangle_a\otimes|0,l\rangle_b\\ |1,k\rangle_a\otimes|0,l\rangle_b\mapsto\cos\theta|1,k\rangle_a\otimes|0,l\rangle_b-\sin\theta|0,k\rangle_a\otimes|1,l\rangle_b\\ |1,k\rangle_a\otimes|1,l\rangle_b\mapsto|1,k\rangle_a\otimes|1,l\rangle_b.\end{cases} \tag{2}$$

The angle θ is proportional to the gating time in which both cells are in active states. The square root of the exchange ($\theta=\pi/4$) is useful in the construction of a controlled NOT gate [28]. Since the exchange gate has a single continuous parameter θ, it should be more powerful than a discrete controlled NOT gate. In other words, it is expected that circuit complexity is reduced. For the sake of the universality of quantum circuits, two-qubit gates for an arbitrary remote pair of qubits must be possible. However, in many physical implementations, this requirement would be very difficult. Although it is possible to arrange multiple controlled NOT operations for adjacent qubits and rotations so that they mimic single operations for a pair of remote qubits, it costs a lot in terms of steps of gating. The exchange operation means $U_{ab}(\pi/2)$ in a narrower sense. This operation is especially convenient since it exchanges the complex amplitudes of two qubits completely in a single step. Thus, the total number of steps necessary for some computational tasks should become much fewer. As easily understood, this interconnection problem is influenced by the average number of connections from a cell. To increase this value, higher-dimensional structures are effective since the average distance between any qubit pair in an N-qubit circuit scales as $N^{1/d}$, where d is the dimensionality of the network.

Next, we consider single-qubit operations. As in the standard scheme, a rotation with an arbitrary angle is facilitated. In our scheme, the rotation about the x, y, and z axes is switched on if and only if the ancilla state is 2, 3, or 4, respectively. Unitary operators are

$$\begin{aligned}R_x(\theta):&|w,2\rangle\mapsto|R_x(\theta)w,2\rangle,\\ R_y(\theta):&|w,3\rangle\mapsto|R_y(\theta)w,3\rangle,\\ R_z(\theta):&|w,4\rangle\mapsto|R_z(\theta)w,4\rangle.\end{aligned} \tag{3}$$

For an arbitrary rotation, only two kinds of rotation with fixed axes, $R_x(\theta)$ and $R_y(\theta)$, are necessary since $R_z(\theta)$ can be synthesized by combining them. However, the full set of

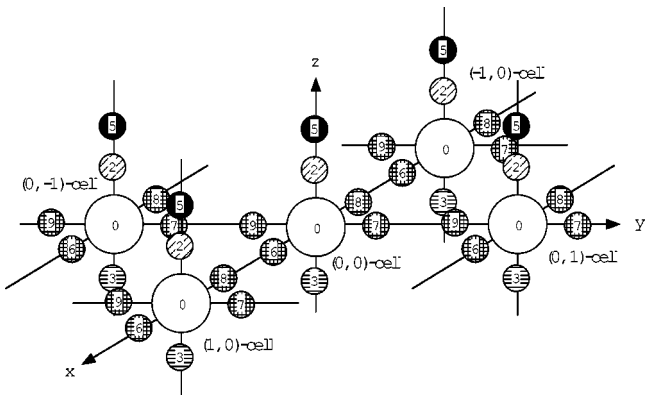

FIG. 2. Example of two-dimensional square lattice version of proposed scheme. Seven ancilla dots are used in each cell. The R_x and R_y dots denoted by 2 and 3 are located along the positive and negative z axes. The measurement dot denoted by 5 is above the R_x dot. The four ancilla dots for the two-bit operation denoted by 6, 7, 8, and 9 are located toward the neighboring cell.

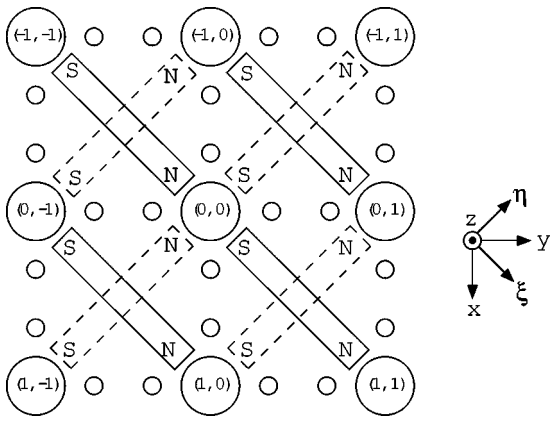

FIG. 3. Proposed configuration of nanoscale ferromagnets embedded in network of Fig. 2. The larger circles are the central columns of cells. The rectangles with the solid (broken) lines indicate ferromagnets in the upper (lower) layer of R_ξ dots (R_η dots). The ferromagnets are magnetized by an external magnetic field toward the positive y direction.

axes of rotation is effective for both the simplicity of circuit design and the reduction of circuit complexity. A local magnetic field can rotate the spin. One possible method is described later.

The single-bit phase shift is a necessary operation for some quantum algorithms. A controlled phase shift, for example, can be constructed simply by using rotation and phase shift. The phase shift $\Phi(\phi)$ is switched on if and only if the ancilla state is 1. The unitary operator is

$$\Phi(\phi):|w,1\rangle\mapsto e^{i\phi}|w,1\rangle. \tag{4}$$

The qubits must be measured at the end or during the course of computations. We implement an ancilla bit 5 for the measurement. First, the qubit is entangled with the ancilla bit. Then measurement of the state of the ancilla becomes equivalent to that of the qubit. A qubit is measured to be $|1\rangle$ if the ancilla state is 5 and $|0\rangle$ if the ancilla state is 0. This procedure is explained later in detail. Thus, in our scheme, only the sequence of π pulses is necessary for operation, except in the final step of the measurement procedure.

Figure 2 shows an example of the proposed scheme with a rather economical cell construction strategy. In this example, only seven ancilla dots are used in each cell. It adopts the design of a two-dimensional square lattice. The R_x and R_y dots denoted by 2 and 3 are located along the positive and negative z axes, respectively. The measurement dot denoted by 5 is above the R_x dot. The R_z and Φ dots are omitted. Ancilla dots for single-bit operations are away from each other and neighboring cells. In contrast, the four ancilla dots denoted by 6, 7, 8, and 9 for two-bit operations are located toward the neighboring cells, like chemical bonds in molecules. The distances between ancilla dots responsible for this operation [e.g., the eighth dot in the (1,0) cell and the sixth dot in the (0,0) cell] are reduced for the kinetic exchange interaction to work. Furthermore, the matrix element for the dipole moments $M_8^{(1,0)}$ between ground state $|w,0\rangle_{(1,0)}$ and active states $|w,8\rangle_{(1,0)}$ and $M_6^{(0,0)}$ between $|w',0\rangle_{(0,0)}$ and active states $|w',6\rangle_{(0,0)}$ is designed so that $|M_8^{(1,0)}|=|M_6^{(0,0)}|$ in order to synchronize the activation. The matrix element for the dipole moment can be tuned by designing the sizes of dots and the distance between them since $M_i\equiv\langle w,i|e\mathbf{r}|w,0\rangle=\int d\mathbf{r}\phi_i(\mathbf{r})e\mathbf{r}\phi_0(\mathbf{r})$, where ϕ_0 and ϕ_i are the wave functions for electrons confined in the main and ith ancilla dots.

As the energy levels differ, ancilla bits can be distinguished by the frequency of their optical π pulse. As the extension of this multiplicity in the wavelength domain, the different dots have different energies whether they are in the same cell or different cells. However, the differences of eigen energy in different cells may be much smaller than those in the same cell since small detuning is sufficient for suppressing Rabi oscillations. This fact will help to save frequency resources. Furthermore, dots in remote cells that have separations larger than the radius of the laser spot may have identical spectra.

A local magnetic field for the $R_{x,y,z}$ dot is realized, of course, simply by placing a nanometer-sized permanent magnet next to the dot. However, since it is hard to shield the magnetic field completely, spins outside the $R_{x,y,z}$ dot can also be influenced by it. To solve this problem, we propose to adopt a special configuration of ferromagnets embedded in our network as shown in Fig. 3. We use $R_{\xi,\eta}$ instead of $R_{x,y}$, where $x=(\xi-\eta)/\sqrt{2}, y=(\xi+\eta)/\sqrt{2}$. Small ferromagnets lie laterally such that they connect the $R_{\xi,\eta}$ dots of diagonally neighboring cells. Thus, local magnetic fields are directed in the positive ξ direction for the upper R_ξ dot layer and positive η direction for the lower R_η dot layer. The magnetization of the small ferromagnets is done by applying an external static magnetic field toward the positive y direction. The leakage of magnetic flux can be made small by reducing the gap between poles. This device structure is not hard to fabricate since we have no semiconductor quantum dots on the top of the ferromagnetic material. We also propose to use high-g-factor material for the $R_{\xi,\eta}$ dots to reduce the effect of leakage of the magnetic field. In a relatively weak mag-

netic field, the electron spin in an $R_{x,y,z}$ dot can make a rapid precession without affecting the spin in other dots with a small g factor. Diluted magnetic semiconductors such as $Ga_xMn_{1-x}As$ are interesting candidates for this purpose, since they can be grown epitaxially on GaAs. Evidence for strong p-d exchange interactions has been suggested theoretically and experimentally. This may support the usage of holes instead of electrons in our cells.

As for the measurement of the qubit, the help of the R_ξ dot is needed along with a measurement dot. The measurement dot must have a lower energy level than the R_ξ dot. The measurement procedure is as follows;

$$|\text{initial}\rangle = c_1|\uparrow,0\rangle + c_2|\downarrow,0\rangle \tag{5}$$

$$\xrightarrow{\pi_1} c_1|\uparrow,2\rangle + c_2|\downarrow,0\rangle \tag{6}$$

$$\xrightarrow{\pi_2} c_1|\uparrow,5\rangle + c_2|\downarrow,0\rangle \tag{7}$$

$$\xrightarrow{\text{measurement}} |\uparrow,5\rangle \text{ or } |\uparrow,0\rangle. \tag{8}$$

First, using a π pulse with a line spectrum tuned to the up-spin level in the R_ξ dot, the corresponding component of the electron wave function is transferred from the main dot to the R_ξ dot: Eq. (6). Next, using a second π pulse, the same component of the electron wave function is transferred from the R_ξ dot to the measurement dot: Eq. (7). Finally, the polarization of the cell is detected by capacitively coupling the central island of a single-electron transistor to the measurement dot: Eq. (8). The entangled state in Eq. (7) is very stable in the sense that the partition of probability among two dots (0 and 5) is not changed by the Coulomb interactions of many electrons flowing through tunnel junctions of the single-electron transistor since direct transfer between these dots is forbidden. Although the phase memory would be lost very quickly in the course of this last step, amplitude memory is sustained until we finally observe the output voltage of the single-electron transistor.

Next, we consider the decoherence characteristics of our cell. The cell state is the vector in product space for the qubit and ancillas. Both freedoms have their specific interaction with the environment. In general, ancilla bits are far more strongly coupled to the environment than the qubit. We neglect the direct coupling of the qubit to its environment and investigate indirect decoherence via a single ancilla bit, for simplicity. As the Hamiltonian for qubit operation, we assume

$$H_{op} = \frac{J}{4}\begin{bmatrix} -1 & 2 \\ 2 & -1 \end{bmatrix} \tag{9}$$

in the Hilbert space $\mathcal{H}_q$ for a qubit. This is a submatrix of an exchange Hamiltonian. The creation operator $a_c^\dagger$, the annihilation operator a_c, and the π pulse operator U_π are

$$a_c^\dagger = \begin{bmatrix} 0 & 1 \\ 0 & 0 \end{bmatrix},\ a_c = \begin{bmatrix} 0 & 0 \\ 1 & 0 \end{bmatrix},\ \text{and}\ U_\pi = \begin{bmatrix} 0 & 1 \\ -1 & 0 \end{bmatrix} \tag{10}$$

in the Hilbert space $\mathcal{H}_a$ for the ancilla with the basis of $|0_a\rangle$ and $|1_a\rangle$. The operation Hamiltonian acting on the product space $\mathcal{H}_q \otimes \mathcal{H}_a$, denoted by a tilde, is

$$\tilde{H}_{op} = \begin{bmatrix} I & 0 \\ 0 & H_{op} \end{bmatrix}, \tag{11}$$

where I is the unit matrix. We examine the following operation procedure:

$$\tilde{\rho}_i = |w,0_a\rangle\langle w,0_a| \xrightarrow{\tilde{U}_\pi} |w,1_a\rangle\langle w,1_a| \xrightarrow[\text{decoherence}]{\tilde{U}_{op}} \tilde{\rho} \xrightarrow{\tilde{U}_\pi} \tilde{\rho}' \xrightarrow{\text{damping}} \tilde{\rho}_f = \rho_f \otimes |0_a\rangle\langle 0_a|, \tag{12}$$

where $\tilde{U}_{op}$ is a unitary evolution generated by $\tilde{H}_{op}$. We assume the π pulse is accurate. In the final step of Eq. (12), just by leaving the cell alone for approximately the same period as the operation, the ancilla bit resets to $|0_a\rangle$. In practice, the density matrix of cells becomes

$$\tilde{\rho}'_{c1} = \rho_{00}\otimes|0_a\rangle\langle 0_a| + \rho_{01}\otimes|0_a\rangle\langle 1_a| + \rho_{10}\otimes|1_a\rangle\langle 0_a| + \rho_{11}\otimes|1_a\rangle\langle 1_a| \xrightarrow{\text{damping}} (\rho_{00}+\rho_{11})\otimes|0_a\rangle\langle 0_a| \equiv \rho_1\otimes|0_a\rangle\langle 0_a|,$$

$$\tilde{\rho}'_{c2} \to \rho_2 \otimes |0_{a1},0_{a2}\rangle\langle 0_{a1},0_{a2}|,$$

$$\tilde{\rho}'_{c3} \to \rho_3 \otimes |0_{a1},0_{a2},0_{a3}\rangle\langle 0_{a1},0_{a2},0_{a3}|, \tag{13}$$

$$\vdots$$

$$\tilde{\rho}'_{cn} \to \rho_n \otimes |0_{a1},0_{a2},\ldots,0_{an}\rangle\langle 0_{a1},0_{a2},\ldots,0_{an}|,$$

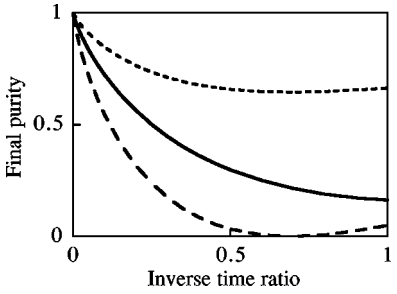

FIG. 4. Final purity s after full spin-flip operation as function of inverse time ratio R_t^{-1} (gating time over coherence time) starting from $|0,0_a\rangle\langle 0,0_a|$ (the solid curve). The dotted curve and broken curve are purities for a simple two-level system starting from $|1\rangle$ and $|0\rangle+|1\rangle$, respectively.

where $\tilde{\rho}'_{cn}$ are density matrices for n cells, ρ_n are density matrices for n qubits, and $|0_{a1},0_{a2},\ldots,0_{an}\rangle$ are the kets of n ancillas. Thus, we are left only with the Hilbert space for qubits disentangled from ancillas. Therefore, we can employ the usual quantum error correction algorithm for qubits to maintain quantum computation. This also supports the contraction of the Hilbert space discussed later and keeps the ancilla bit as a classical bit. The second step in the procedure of Eq. (12) is described by a von Neumann equation with dissipation terms:

$$\dot{\tilde{\rho}}=-\frac{i}{\hbar}[\tilde{H}_{op},\tilde{\rho}]-\frac{1}{2\tau_a}\{[a_c^\dagger,a_c\tilde{\rho}]+\text{H.c.}\}, \qquad (14)$$

where τ_a is the coherence time for an ancilla bit. Figure 4 shows the final purity $S=T_r\rho_f\ln\rho_f+1$after a full spin-flip operation as a function of the inverse time ratio R_t^{-1} (gating time over coherence time), starting from $|0,0_a\rangle\langle 0,0_a|$ (the solid curve). The broken curve and dotted curve are final purities for a simple two-level system starting from $|1\rangle$ and $(|0\rangle+|1\rangle)/\sqrt{2}$, respectively. Thus, the indirect spin decoherence rate is on the same order as the ancilla decoherence rate. The mechanism of indirect decoherence is as follows. In the course of spin rotation, the orbital relaxation redistributes the density matrix element in an asymmetrical way into two submatrices $|0_a\rangle\langle 0_a|$ and $|1_a\rangle\langle 1_a|$. As a result, the final spin state traced over the orbital degree of freedom becomes no longer a pure state. In the case of the present relaxation model, no entanglement between spin and orbital is generated, since both spin rotation and orbital relaxation are ''local'' operations for each single qubit. However, this decoherence occurs only in a gated period. If the duty ratio R_d of active time to total time is much smaller than unity, the effective decoherence time τ_a/R_d becomes very long. In quantum circuits, only single- and two-qubit gates are used. If parallelism is not used, in an N-qubit circuit, the duty ratio ranges from $1/N$ to $2/N$. Thus, the larger the circuit, the more efficient this scheme becomes. The disadvantage of excess decoherence due to the incorporation of ancilla bits should be largely compensated.

Now, we discuss the state space of the ancilla. In the most general case, the Hilbert space of our cell is spanned by the kets

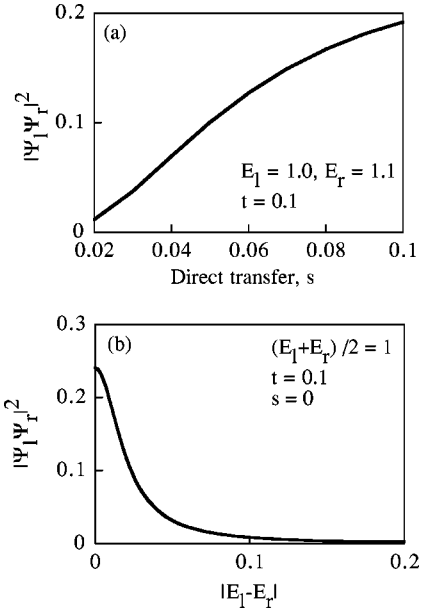

FIG. 5. Product of probabilities of occupation in both dots as functions of (a) direct transfer s and (b) energy difference of levels $|E_l-E_r|$ in both dots.

$$|w,z_1,z_2,\ldots,z_m\rangle=|w\rangle\otimes|z_1\rangle\otimes|z_2\rangle\otimes\cdots\otimes|z_m\rangle, \qquad (15)$$

where $|w\rangle$ denotes the qubit state and $|z_k\rangle$ $(k=1,\ldots,m)$ are the states of ancilla bits, all of which may correspond to different degrees of freedom. Thus, our cell is a 2^{m+1}-level system. However, by adopting a specific physical design and operation scheme, we can ignore most parts of the Hilbert space. This space contraction is made in two steps. First, state vectors are restricted to

$$\begin{aligned}
|w,0,0\rangle&=|w,0,0,\ldots,0\rangle,\\
|w,z_1,1\rangle&=|w,z_1,0,\ldots,0\rangle,\\
|w,z_2,2\rangle&=|w,0,z_2,\ldots,0\rangle,\\
&\vdots\\
|w,z_m,m\rangle&=|w,0,0,\ldots,z_m\rangle,
\end{aligned} \qquad (16)$$

where $z_1,z_2,\ldots,z_m\neq 0$. That is, we ignore states like $|w,0,\ldots,0,z_k,0,\ldots,0,z_l,0,\ldots,0\rangle$. This means that the cell is reduced to the product of a qubit and an $(m+1)$-level system such that the possibility of a large amplitude in more than two excited levels is neglected. In order to find the necessary conditions for this assumption to hold, as a simple model for a coupled-dot system, we examine a three-site, one-electron (i.e., three-level) system

$$\begin{aligned}
\hat{H}=&E_l n_l+E_c n_c+E_r n_r+t(a_l^\dagger a_c+a_c^\dagger a_l-a_r^\dagger a_c-a_c^\dagger a_r)\\
&+s(a_l^\dagger a_r+a_r^\dagger a_l),
\end{aligned} \qquad (17)$$

where the subscripts l, c, and r mean the left, center, and right dots. This is because it is neither easy nor revealing to work on the complex three-dimensional (3D), three-dot full Hamiltonian. However, the 3D model may be simplified into

a site model, if we make the appropriate correspondence in energies and physical sizes between the two models [30]. In the following, we use specific parameter values in the site model that correspond to diameters of about 50, 35, and 34 nm for central, left, and right dots and dot spacings of less than 10 nm. With these parameter values, the level spacing becomes about 0.005 eV, which is 1.2 THz in frequency and 250 μm in wavelength. Figure 5 shows the product of the probabilities of occupation in two different ancilla dots for one of the excited levels as functions of (a) direct transfer s and (b) the difference of site energies in both dots $|E_l - E_r|$. From these results, we are led to simple conditions: (1) direct transfer s between different ancilla dots must be very small; (2) site energies of ancilla dots must have a sufficiently large difference (5–10 % in this example). Both conditions determine the upper limit of the number of ancilla bits in a cell. It should be less than about 10. If the number of ancilla bits in a cell is small, the first condition can be fulfilled easily by the appropriate arrangement of ancilla dots since the tunneling probability decreases exponentially with the barrier thickness.

The second contraction is due to the operation scheme where ancilla bits are used not as qubits but as classical bits, and we always put the cell in either the completely active $|1\rangle$ or completely sleeping $|0\rangle$ state and not in a superposed state. Therefore, all z_k take values 0 or 1. As a result, we may consider only

$$\begin{aligned} |w,0\rangle &= |w,0,0,...,0\rangle, \\ |w,1\rangle &= |w,1,0,...0\rangle, \\ |w,2\rangle &= |w,0,1,...0\rangle, \\ &\vdots \\ |w,m\rangle &= |w,0,0,...,1\rangle. \end{aligned} \tag{18}$$

Thus, the cell state is expressed by a qubit state $|w\rangle$ and an integer k running from 0 to m that indicates the ancilla states. For this condition to hold, the π pulse for the activation of the ancilla must be accurate in frequency and duration. Furthermore, damping is utilized to ''refresh'' the ancilla state. This technique has already been explained.

In conclusion, a spin quantum network structure with ancilla bits in every cell was proposed. The whole circuit works with the help of only external optical pulse sequences. External switchings of electric and magnetic field are not necessary. In operation, an ancilla bit is activated and autonomous single- and two-bit operations are performed. In the sleep mode of a cell, the decoherence of a qubit is negligibly small. In the active state, indirect decoherence due to the coupling of an ancilla bit to its environment is of the same order of magnitude as simple ancilla decoherence. However, the fact that the duty ratio of each bit scales as N^{-1} improves the effective decoherence time. A device structure using a quantum-dot array with possible operation and measurement schemes was also proposed.

[1] D. Deutsch, Proc. R. Soc. London, Ser. A **400**, 97 (1985); **425**, 73 (1989).

[2] D. Deutsch and R. Jozsa, Proc. R. Soc. London, Ser. A **439**, 553 (1992).

[3] P. W. Shor, in *Proceedings of the 35th Annual Symposium on Foundations of Computer Science*, edited by Goldwasser (IEEE Computer Society, Los Alamitos, CA, 1994), p. 124.

[4] L. K. Grover, Phys. Rev. Lett. **79**, 325 (1997).

[5] J. I. Cirac and P. Zoller, Phys. Rev. Lett. **74**, 4091 (1995).

[6] D. G. Cory, A. F. Fahmy, and T. F. Havel, in *Proceedings of the Workshop on Physics and Computation (PhysComp 96)*, edited by T. Toffoli *et al.* (New England Complex Systems Institute, Cambridge, MA, 1996), p. 87.

[7] N. A. Gershenfeld, I. Chuang and S. Lloyd, in *Proceedings of the Workshop on Physics and Computation (PhysComp96* (Ref. [6]), p. 134.

[8] N. A. Gershenfeld and I. Chuang, Science **275**, 350 (1997).

[9] D. G. Cory, A. F. Fahmy, and T. F. Havel, Proc. Natl. Acad. Sci. U.S.A. **94**, 1634 (1997).

[10] J. A. Jones, M. Mosca, and R. H. Hansen, Nature (London) **393**, 344 (1998).

[11] M. Reck, A. Zeilinger, H. J. Bernstein, and P. Bertani, Phys. Rev. Lett. **73**, 58 (1994).

[12] N. J. Cerf, C. Adami, and P. G. Kwiat, Phys. Rev. A **57**, R1477 (1998).

[13] S. Takeuchi, in *Proceedings of the Workshop on Physics and Computation (PhysComp96)* (Ref. [6]), p. 299.

[14] B. E. Kane, Nature (London) **393**, 133 (1998).

[15] A. Barenco, D. Deutsch, A. Ekert, and R. Jozsa, Phys. Rev. Lett. **74**, 4083 (1995).

[16] S. Tarucha, D. G. Austings, T. Honda, R. J. van der Hage, and L. P. Kouwenhoven, Phys. Rev. Lett. **77**, 3613 (1996).

[17] T. Fujisawa, T. H. Oosterkamp, W. G. van der Wiel, B. W. Broer, R. Aguado, S. Tarucha, and L. P. Kouwenhoven, Science **282**, 932 (1998).

[18] T. H. Oosterkamp, T. Fujisawa, W. G. van der Wiel, K. Ishibashi, R. V. Hijman, S. Tarucha, and L. P. Kouwenhoven, Nature (London) **395**, 873 (1998).

[19] P. W. Shor, Phys. Rev. A **52**, R2493 (1995).

[20] A. M. Steane, Phys. Rev. Lett. **77**, 793 (1996).

[21] A. R. Calderbank and P. W. Shor, Phys. Rev. A **54**, 1098 (1996).

[22] A. M. Steane, Proc. R. Soc. London, Ser. A **452**, 2551 (1996).

[23] R. Laflamme, C. Miquel, J. P. Paz, and W. H. Zurek, Phys. Rev. Lett. **77**, 198 (1996).

[24] C. H. Bennett, D. P. DiVincenzo, J. A. Smolin, and W. K. Wootters, Phys. Rev. A **54**, 3824 (1996).

[25] D. P. DiVincenzo and P. W. Shor, Phys. Rev. Lett. **77**, 3260 (1996).

[26] A. M. Steane, Phys. Rev. Lett. **78**, 2252 (1997).

[27] J. Preskill, Proc. R. Soc. London, Ser. A **454**, 385 (1998).

[28] D. Loss and D. P. DiVincenzo, Phys. Rev. A **57**, 120 (1998).

[29] G. Burkard, D. Loss, and D. P. DiVincenzo, Phys. Rev. B **59**, 2070 (1999).

[30] K. Nomoto, R. Ugajin, T. Suzuki, and I. Hase, J. Appl. Phys. **79**, 291 (1996).